JVSTB Journal of Vacuum Science & Technology B

Effects of stress on electron emission from nanostructured carbon materials

C. H. P. Poa, R. G. Lacerda, D. C. Cox, F. C. Marques, and S. R. P. Silva

Citation: Journal of Vacuum Science & Technology B **21**, 1710 (2003); doi: 10.1116/1.1591747
View online: http://dx.doi.org/10.1116/1.1591747
View Table of Contents: http://scitation.aip.org/content/avs/journal/jvstb/21/4?ver=pdfcov
Published by the AVS: Science & Technology of Materials, Interfaces, and Processing

Effects of stress on electron emission from nanostructured carbon materials

C. H. P. Poa[a)]
Advanced Technology Institute, School of Electronics and Physical Sciences, University of Surrey, Guildford, Surrey GU2-7XH, United Kingdom

R. G. Lacerda
Advanced Technology Institute, School of Electronics and Physical Sciences, University of Surrey, Guildford, Surrey GU2-7XH, United Kingdom and Universidade Estadual de Campinas, Unicamp, Instituo de Fisica "Gleb Wataghin," 13083-970, Campinas-SP, Brazil

D. C. Cox
Advanced Technology Institute, School of Electronics and Physical Sciences, University of Surrey, Guildford, Surrey GU2-7XH, United Kingdom

F. C. Marques
Universidade Estadual de Campinas, Unicamp, Instituo de Fisica "Gleb Wataghin," 13083-970, Campinas-SP, Brazil

S. R. P. Silva
Advanced Technology Institute, School of Electronics and Physical Sciences, University of Surrey, Guildford, Surrey GU2-7XH, United Kingdom

(Received 12 December 2002; accepted 19 May 2003; published 31 July 2003)

The electron field emission properties of highly graphite like (sp^2 rich) amorphous carbon films have been investigated. These films were prepared by dual ion beam-assisted deposition technique, where the assisting energies were varied from 0 to 800 eV. Threshold fields as low as 8 V/μm is observed at an assisting energy of 400 eV, which is comparable to the best threshold fields observed in high sp^3 carbon films. Surface nanostructures are found on these films during growth, but are thought not to be the primary reason for the observed low threshold fields. The combination of a highly graphite-like structure with a high intrinsic compressive stress and a high local (electronic) density, obtained from x-ray photoelectron spectroscopy, is identified as the source for the field enhancement. The controllable stress is thought to modify the band structures of the graphite-like sp^2 rich component in the films, which results in high dielectric inhomogeneity. This analysis is in agreement with the concept of an internal or nongeometric field enhancement from sp^2 nanostructures within the carbon thin films. The effect of stress induced band structure modification can also be extended to explain the field emission behavior of carbon nanotubes under stress. [DOI: 10.1116/1.1591747]

Amorphous carbon (a-C) thin films in the hydrogen-free form can exist in the graphite-like or tetrahedral states depending on the sp^3 or sp^2 hybridization within the films. Films with high sp^3 concentration are highly tetrahedral amorphous carbon (TAC) with diamond-like properties such as high band gap and high hardness. Graphite-like a-C (GAC) films on the other hand have very similar properties to graphite such as low or zero band gap and high conductivity. One of the interesting properties of a-C films is that it possesses a relatively high intrinsic stress within the material. The mechanisms for generating such a high intrinsic compressive stress have been explained due to the energy of the ion bombardment during the deposition process causing a sp^2 to sp^3 bonds transition when a critical stress of $\sim$5 GPa is maintained within the film.[1,2] The subimplantation model, where in the presence of ion bombardment the formation of sp^2 and sp^3 bonds just below the growing surface is well accepted,[3,4] in which the densification is due mainly to the presence of sp^3 bonds. Recent studies have shown that it is possible to produce a-C thin films with high sp^2 concentrations that exhibit local density, hardness, and intrinsic stress similar to those of TAC films.[5] These have been attributed to the densification of the film during the "knock-on" process of the carbon atoms beneath the surface. The densification of the carbon film occurs in relation with the reduction of the distance between sp^2 clusters. From a tribological viewpoint, high stress is undesirable due to adhesion problems with the substrate. However, it is well know that the electronic properties of carbon-based materials change when the carbon phase is under high pressure/stress. Reports have shown that amorphous carbon under high pressure can result in an increase in the film conductivity.[6] By applying pressure to a material one can modify its electronic properties, e.g., band structure, resistivity, Fermi level.[7,8] It is therefore of scientific interest to study the effects of high intrinsic stress on the electronic properties of GAC films.

Early reports postulated that the emission threshold field (E_{th}) is controlled by the sp^3 content.[9] However, more re-

[a)]Electronic mail: patrick.poa@eim.surrey.ac.uk

cent studies[10,11] have demonstrated that the distribution of the sp^2 C sites can be a dominant factor in giving rise to the high internal field enhancement within the *a*-C structure. In a recent article, Carey *et al.*[10] explained the field enhancement of *a*-C:H films in terms of the dielectric inhomogeneities between the sp^2 and sp^3 phases, where the origin of the field enhancement was based on the proximity of the conductive sp^2 clusters within the film giving rise to electromagnetic field perturbations. The effects of stress on these sp^2 clusters could therefore play an important role in the field emission properties.

The *a*-C films were deposited by an ion beam assisted deposition technique using two Kauffman ion sources. A high-purity graphite target (99.99%) is sputtered by different noble gas ions at a beam voltage of 1500 V, using a total beam current of 90 mA, while the second Kauffman source is used to ion irradiate the growing *a*-C thin film surface. Films were prepared separately with neon, argon, and krypton gases introduced in both Kauffman sources. The substrate holder allows the substrate temperature to be heated up to 1000 °C. This removable holder also allows easy *in situ* transfer of the samples to an ultraviolet/x-ray photoelectron spectroscopy (UPS/XPS) analysis system. All films were prepared at 150 °C applying an ion beam assisting energy (AE) in the range 0–800 eV. After the deposition, the samples were transferred, under vacuum, to the ultrahigh vacuum chamber (pressure$<10^{-7}$ Pa) for *in situ* photoelectron spectroscopy measurements (XPS and UPS). Electron energy loss spectroscopy (EELS) was also performed to obtain the plasmon loss and the concentration of sp^2 sites using a Philips CM 200 microscope with an imaging Gatan PEELS system. Stress measurements were performed using films deposited on *c*-Si bars, applying an optical bending beam method to determine the radius of curvature of the film/substrate composite.[12] Stress measurements were taken from *a*-C films deposited on $4\times25\times0.4$ mm^3 (111) *c*-Si bars, by determining the radius of curvature of the film/substrate composite. An apparatus based on the detection of a He–Ne laser was used for this purpose. The use of two laser beams allows static measurements. In addition, it substantially reduces the time spent on each measurement, making it possible to continuously acquire data as a function of temperature. The stress of a thin film, deposited on a substrate, which has a length that is much greater than its width and thickness, is given by the modified Stoney's equation[13]

$$\sigma=\left[\frac{E_s}{1-\nu_s}\right]\left(\frac{t_s^2}{6t_f}\right)\left(\frac{1}{R}-\frac{1}{R_0}\right),$$

where E, ν, and t are the Young's modulus, Poisson's ratio, and thickness, respectively. The superscripts s and f refer to substrate and film. R_0 and R are the radii of curvature of the substrate before and after the film is deposited. The film thickness was about 100 nm. The field emission (FE) characteristics of these films were determined using a sphere-to-plane technique. The anode in this case is a 5 mm stainless-steel ball separated from the film surface at a gap of 20–50 μm in a vacuum better than 4×10^{-6} mbar. Some conditioning of these films were required, but the initiation fields recorded were significantly lower than those reported elsewhere.[14] The importance of conditioning and thereby creation of localized FE has been studied extensively and is an accepted phenomenon in "resistive" and more diamondlike amorphous carbon films. The creation of surface features and conducting channels within the film are a possible result of the conditioning cycle. But, in our highly conductive "graphite-like" *a*-C films there is no requirement for large conditioning fields, and little evidence of any surface features subsequent to field emission. The threshold field (E_{th}) is defined as the microscopic electric field where an emission current of 1 nA is observed. An emission current is preferred to compare threshold fields as it removes any ambiguity of using an emission area from which electrons are emitted from these flat cathodes.

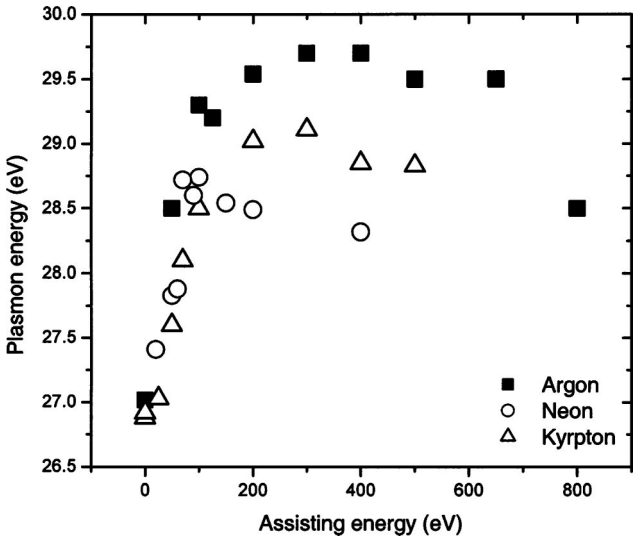

FIG. 1. Variation of the plasmon energy of the *a*-C film as a function of the assisting energy with different noble gases (■) argon, (○) neon, and (△) krypton.

Analysis based on XPS, density (from Rutherford backscattering spectrometry) and Raman analysis indicate that the material is composed of a highly compressed and dense sp^2 network.[5] These characterizations are in agreement with the high values of sp^2 bonds ($\sim$90%), obtained from EELS, found for all the samples. The UPS (top of the valence band) and band gap measurements, which shows an absence of a band gap in all the films indicate the graphitic nature of the films. The changes on the plasmon energy (from the C 1*s* plasmon peak) as a function of assisting energy with different ions are shown in Fig. 1. In order to probe the local/microscopic density, the plasmon energy was measured by XPS. The plasmon energy peak is a measure of the inelastic scattering of the C 1*s* electrons before leaving the sample. The plasmon energy is related to the mass density assuming a free electron model with the plasmon energy proportional to the square root of the effective valence electron density. The densities obtained by this method are known to overestimate the real value.[15] In this work, we will not be attempting to determine the absolute electronic density but investi-

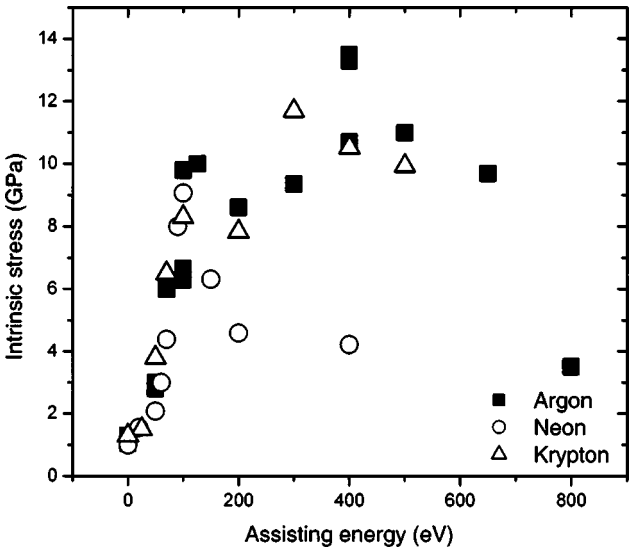

FIG. 2. Variation of the intrinsic stress of the *a*-C film as a function of the assisting energy with different noble gases (■) argon, (○) neon, and (△) krypton.

gating the relative variation of plasmon energy to the assisting energy. The plasmon energy increases observed in the films are seen to be independent of the assisting energy for all three types of ions (Ne^+, Ar^+, and Kr^+) from 0 to 800 eV AE. For Ne^+ assisted films, the plasmon energy falls off after reaching a maximum of 28.7 eV at 100 eV AE. Similar trends were observed for Ar^+ and Kr^+ assisted films, with maximum plasmon energies of 29.5 and 29.1 eV at around 400 eV AE, respectively. The intrinsic stress as a function of the AE for different ions is shown in Fig. 2. The variation of the intrinsic stress is very similar to the plasmon energy. For the Ne^+ assisted films, the stress increased to a maximum of 10 GPa at AE of about 100 eV and decreases to 4.3 GPa at 200 eV. For Ar^+ and Kr^+ assisted films, the intrinsic stress increased to 14 and 12 GPa at AE of 400 and 300 eV, respectively. The plasmon energy and intrinsic stress both show very interesting and similar variation with the AE and the assisting ions. At AE below 100 eV, the mechanism that controls the properties of these films seems to be independent of the mass and energy of the ions. However, above 100 eV of AE, the differences are more clearly seen between different ions. This may be explained by the effect that the ion mass starts to exert more influence on the properties of the films above 100 eV AE.

It is worth noting that the maximum value of plasmon energy and instrinsic stress observed in the Ar^+ ion assisted film of ~29.5 eV and ~12 GPa is similar to those observed in TAC.[16,17] To illustrate high intrinsic stress and high local density within a highly graphitic matrix, Fig. 3 shows a cross-sectional view of the possible arrangement of sp^2 clusters within the thin film. In Fig. 3(a), the low intrinsic stress and low local density will result in the sp^2 clusters being far apart. However, the sp^2 clusters becomes very closely packed together when subject to high stress and increased local density in the film [Fig. 3(b)]. This is also in agreement

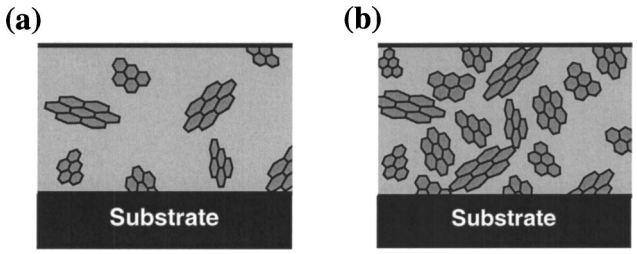

FIG. 3. Illustration of the possible arrangement of the sp^2 clusters in the film: (a) film with low intrinsic stress and low local electronic density and (b) film with high intrinsic stress and high local electronic density.

with the sheet resistivity measurements, which show a huge decrease of the resistivity from 0.03 to 0.002 Ω cm for the Ar^+ assisted films when the AE is increased from 0 to 400 eV. In addition, it is important to stress that the R_S values of 0.09 Ω cm are comparable to the sheet resistance observed in the *c*-axis orientation of graphite.

Scanning tunneling microscopy (STM) images of the *a*-C grown with Ar at the assisting energy in Fig. 4(a) 0 eV, (b) 70 eV, (c) 400 eV, and (d) 650 eV were examined. Highly conductive nanostructures are observed on the surface of these films. The graphitic clusters recorded are not distorted but oriented in different directions. The measurements for the STM are conducted at a fixed current mode of 1 pA. The variation in height or topology of the film is correlated to the changes in conductivity across the film. The shape and sizes of these nanostructures are dependent on the assisting energy of the Ar gas. In the case without assisting energy, the nanostructures are small and randomly located. As the assisting energy increases at 70 eV, the nanostructures becomes bigger and more dense. At assisting energies of 400 eV, the density increases and these nanostructures become well aligned. A similar result was reported by Schwan *et al.* for their GAC films when subject to high intrinsic stress.[2] However, with increasing energy at 650 eV, the bombardment of assisting ions is too energetic, hence leading to the nanostructures becoming smaller. An analysis of Fig. 4(c) shows that the nanostructures at a high assisting energy are well aligned and dense due to the intense Ar^+ ions introduced during growth. It is possible that the stress within the sp^2 rich segments also cause some of the contrast seen in these films by altering the band structure of the nanostructured graphite. On the other hand, when no assisting is present, Fig. 4(a) shows that the formation of these nanoclusters is random, less conductive, and smaller when compared to those with assisting energy ion bombardment. The highly conductive nanostructures agree well with the R_S (0.09 Ω cm) measurements and also supporting the sp^2 character of the films. It should be noted that highly comparable values of R_s to those of graphite in the disordered nanostructured material adds further credence to the view that electron density increases must be taking place microscopically in the sp^2 rich clusters. Further transmission electron microscopy results show these GAC film contain crystalline nanostructures embedded in an amorphous matrix.

The variation of the field emission threshold field (E_{th}) as

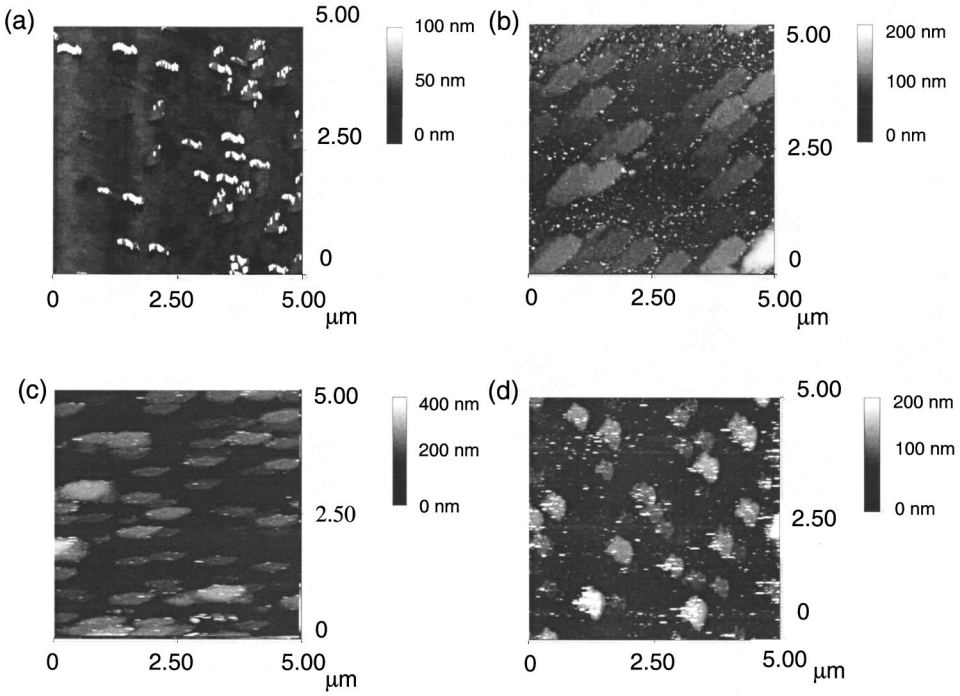

FIG. 4. High resolution STM image of the surface of a-C film grown at an assisting energy of: (a) 0 eV, (b) 70 eV, (c) 400 eV, and (d) 650 eV with argon as assisting noble gas. Highly conductive nanostructures uniformly formed on the surface.

a function of the assisting energy for different assisting ions is shown in Fig. 5. The E_{th} is found to vary in a very similar manner to those of the intrinsic stress and plasmon energy. With no assisting energy, the threshold field reaches a value as high as E_{th} of $\sim 50\ \mathrm{V}/\mu\mathrm{m}$. As the assisting energy increases, E_{th} decreases to values as low as $8\ \mathrm{V}/\mu\mathrm{m}$ at an assisting energy of 400 eV (Ar^+). Further increases in the assisting energy result in the subsequent increase in E_{th} to about $38\ \mathrm{V}/\mu\mathrm{m}$ at 800 eV. It is important to note that the lowest E_{th} is observed in the film with the highest intrinsic stress (~ 12 GPa) and highest local electron density (~ 29.5 eV). In general, all noble gases show a minimum E_{th} similar to the trend of the intrinsic stress. This is very important since it indicates that the internal stress may be controlling the electron FE process. Furthermore, the STM images also show that at 400 eV (Ar) film has the densest sp^2 clustering on its surface. However, thus far it is not clear whether the low threshold observed has its origin due to the stress of the nanostructures at the surface or to the stress of the dense graphitic clusters within the bulk. In atomic force microscopy, surface morphology studies on films grown at 400 eV show surface protrusions of around 50 nm in height and 150 nm in diameter which could not be the reason for the measured low threshold field as a result of high enhancement factors due to surface nanostructures ($\beta = h/r$). In addition, there are no distinct features found on the sample surface after field emission tests that can account for the high field enhancement and low threshold fields measured.

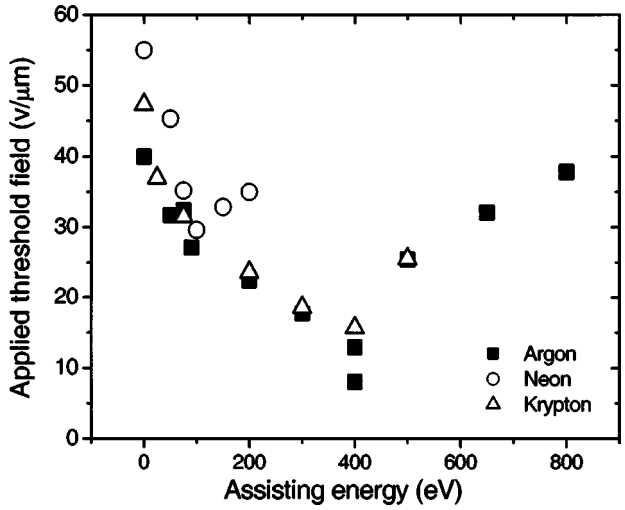

FIG. 5. Variation of threshold electric field as a function of the assisting energy with different noble gases: (■) argon, (○) neon, and (△) krypton.

The low threshold FE characteristics of these highly graphitic a-C films can be influenced by: (1) the high intrinsic stress which influences the band structure of the sp^2 nanostructures; (2) high stress together with high local density allows the highly sp^2 nanostructured regions to be brought closer together (this could create a source of high electric field enhancement);[10] or (3) a combination of both of the above reasons.

The effect of stress/pressure induced band structure modification has been observed in graphite. The work by Ahuja *et al.*[18] shows that the lattice constant c/a subject to 10 GPa hydrostatic pressure results in the reduction in the c/a ratio from 2.72 to 2.42. To have an idea of how significant the reduction between the distances of the graphite planes on the electronic properties, we applied a simple two-band model[19] for the electrical conductivity in the basal plane of graphite. In this model, the concentration of electrons is

$$n_e = \frac{8\pi m_e^* kT}{\hbar^2 c} \ln[1 + \exp\ \eta/kT],$$

where c is the interplanar distance and η is the chemical potential. Assuming band overlap and m_e^* is the effective mass of an electron, this two-band model indicates that the decrease of c can lead to the increase of the electron concentration, which can benefit the electron emission process by providing a larger pool of electrons or lower barrier for emission. According to the hydrostatic experiment by Lynch and Drickamer on graphite,[20] by applying a pressure of 12 GPa on a microcrystalline graphite sample, there is a 15% decrease in the distance between the planes. It should be noted that the pressure applied is comparable to the compressive stress found in the samples shown in Fig. 2.

In this article we propose that the absolute E_{th} value is significantly influenced by the high stress and local density, bringing the nanostructured graphitic carbon closer together. The large and densely populated sp^2 clusters have the advantage of inducing a nongeometric field enhancement within the film by having the clusters close together. Recently, Carey *et al.*[10] suggested that the field enhancement could be attributed to differences in the dielectric and conductive properties of sp^2 clusters surrounded by the more insulating sp^3 matrix. The dielectric mismatch between these two phases can have a significant field enhancement if the conductive sp^2 clusters are closely spaced. For example, Chaumet and Dufour[21] calculated the field enhancement based on two spheres with conductivity of gold. By having a separation distance of 5 nm apart, an enhancement of 56 can be achieved, and a β of 400 is obtained when these clusters approach a separations of 1 nm. Although the conductivity of the sp^2 nanostructures may not be as high as gold, based on the modified band structure arrangement due to high internal stresses, the model presented above may not be far from wrong. All evidence appears to support a field enhancement process based on proximity effects of conductive sp^2 clusters giving rise to electromagnetic modifications of field lines in a highly localized region.

It is also interesting to note that the effect of stress could also be applied to carbon nanotubes. Recent work from Heyd *et al.*[22] on the band gap of nanotubes shows linear variations with stress, where a variation of $|dE_{\text{gap}}/d\sigma| = 10.7$ meV/GPa was measured. At a stress, $|\sigma| \sim 10$ GPa a semiconductor to metal transition is predicted. Therefore, the arguments relating to stress and field emission in this article may also be applicable to the field emission behavior of carbon nanotubes, where localized stress in the CNT may arise due to the pentagonal structures or defects within the nanotubes themselves.

In conclusion, the FE from a sp^2 rich amorphous carbon film has been investigated. These dense GAC films with high sp^2 concentration have shown that low threshold fields of 8 V/μm can be achieved. The STM images show conductive nanostructures on the surface of the films. The surface protrusions do not adequately explain the measured low E_{th}. The field emission characteristics of these films have been explained in term of the high sp^2 concentration, together with the high intrinsic stress modifying the electronic band structure of the film/graphitic nanostructures. This work indicates that by careful control of the stress in nanostructured materials custom designed cathodes can be manufactured and the research opens the doors to a class of cold cathode devices that can be used as sensors and other devices.

The authors would like to acknowledge the financial support received from the EPSRC CBE programme and Portfolio Partnership.

[1] D. R. McKenzie, D. Muller, and B. A. Pailthope, Phys. Rev. Lett. **67**, 773 (1991).
[2] J. Schwan, S. Ulrich, T. Theel, H. Roth, H. Ehrhardt, P. Becker, and S. R. P. Silva, J. Appl. Phys. **82**, 6024 (1997).
[3] Y. Lifshitz, S. R. Kasi, J. W. Rabalais, and W. Eckstein, Phys. Rev. B **41**, 10468 (1990).
[4] J. Robertson, Diamond Relat. Mater. **2**, 984 (1993).
[5] R. G. Lacerda, P. Hammer, C. M. Lepienski, F. Alvarez, and F. C. Marques, J. Vac. Sci. Technol. A **19**, 971 (2001).
[6] S. Bhattacharyya and S. V. Subramanyam, Appl. Phys. Lett. **71**, 632 (1997).
[7] C. Kilic, H. Mehrez, and S. Ciraci, Phys. Rev. B **58**, 7872 (1998).
[8] C. Uher, R. L. Hockey, and E. Ben-Jacob, Phys. Rev. B **35**, 4483 (1987).
[9] B. S. Satyanarayana, A. Hart, W. I. Milne, and J. Robertson, Appl. Phys. Lett. **71**, 1430 (1997).
[10] J. D. Carey, R. D. Forrest, and S. R. P. Silva, Appl. Phys. Lett. **78**, 2339 (2001).
[11] A. Illie, C. Ferrari, T. Yagi, and J. Robertson, Appl. Phys. Lett. **76**, 2627 (2000).
[12] M. M. de Lima, Jr., R. G. Lacerda, J. Vilcarromero, and F. C. Marques, J. Appl. Phys. **86**, 4936 (1999).
[13] R. W. Hoffman, in *Physics of Thin Films*, edited by G. Hass and R. E. Thun (Academic, New York, 1966), Vol. 3, pp. 211–273.
[14] J. D. Carey and S. R. P. Silva, Appl. Phys. Lett. **78**, 347 (2001).
[15] P. Hammer, N. M. Victoria, and F. Alvarez, J. Vac. Sci. Technol. A **18**, 2277 (2000).
[16] Y. Lifshitz, G. D. Lempert, E. Grossman, L. Avigal, C. Uzan-Saguy, R. Kalish, J. Khlik, D. Marton, and J. W. Rabalais, Diamond Relat. Mater. **4**, 318 (1995).
[17] P. J. Fallon, V. S. Veerasamy, C. A. Davis, J. Robertson, G. A. J. Amaratunga, W. I. Milne, and J. Koskinen, Phys. Rev. B **48**, 4777 (1993).
[18] R. Ahuja, S. Auluck, J. Trygg, J. M. Wills, O. Eriksson, and B. Johansson, Phys. Rev. B **51**, 4813 (1995).
[19] W. N. Reynolds and P. R. Goggin, Philos. Mag. **5**, 1049 (1960).
[20] R. W. Lynch and H. G. Drickamer, J. Chem. Phys. **44**, 181 (1966).
[21] P. C. Chaumet and J. P. Dufour, J. Electrost. **43**, 145 (1998).
[22] R. Hryd, A. Charlier, and E. Mcrae, Phys. Rev. B **55**, 6820 (1997).